

## Transparent electromagnetic shielding enclosure with CVD graphene

Yu-Tong Zhao, Bian Wu, Yu Zhang, and Yang Hao

Citation: *Applied Physics Letters* **109**, 103507 (2016); doi: 10.1063/1.4962474

View online: <http://dx.doi.org/10.1063/1.4962474>

View Table of Contents: <http://scitation.aip.org/content/aip/journal/apl/109/10?ver=pdfcov>

Published by the [AIP Publishing](#)

---

### Articles you may be interested in

[X-band frequency response and electromagnetic interference shielding in multiferroic BiFeO<sub>3</sub> nanomaterials](#)

*Appl. Phys. Lett.* **109**, 142904 (2016); 10.1063/1.4964383

[A theory of electrical conductivity, dielectric constant, and electromagnetic interference shielding for lightweight graphene composite foams](#)

*J. Appl. Phys.* **120**, 085102 (2016); 10.1063/1.4961401

[Dielectric properties of glassy disaccharides for electromagnetic interference shielding application](#)

*J. Appl. Phys.* **118**, 184102 (2015); 10.1063/1.4935271

[Frequency selective microwave absorption induced by controlled orientation of graphene-like nanoplatelets in thin polymer films](#)

*Appl. Phys. Lett.* **105**, 103105 (2014); 10.1063/1.4895674

[Electromagnetic absorption and shielding behavior of polyaniline-antimony oxide composites](#)

*AIP Conf. Proc.* **1512**, 1218 (2013); 10.1063/1.4791489

---

A promotional banner for Applied Physics Reviews. On the left is a small image of a journal cover titled 'AIP Applied Physics Reviews' featuring a diagram of a layered structure. The main text 'NEW Special Topic Sections' is in large white font on a blue background with a light flare. Below this, 'NOW ONLINE' is in yellow, followed by 'Lithium Niobate Properties and Applications: Reviews of Emerging Trends' in white. The AIP Applied Physics Reviews logo is in the bottom right corner.

**NEW Special Topic Sections**

**NOW ONLINE**  
Lithium Niobate Properties and Applications:  
Reviews of Emerging Trends

**AIP** Applied Physics  
Reviews

# Transparent electromagnetic shielding enclosure with CVD graphene

Yu-Tong Zhao,<sup>1</sup> Bian Wu,<sup>1,2,a)</sup> Yu Zhang,<sup>1</sup> and Yang Hao<sup>2,a)</sup>

<sup>1</sup>National Key Laboratory of Antennas and Microwave Technology, School of Electronic Engineering, Xidian University, Xi'an 710071, China

<sup>2</sup>School of Electronic Engineering and Computer Science, Queen Mary University of London, London E1 4NS, United Kingdom

(Received 5 June 2016; accepted 29 August 2016; published online 9 September 2016)

Cavity resonant modes of shielding enclosure for housing electronic circuits may cause electromagnetic interference (EMI). Here, we present an effective approach by using graphene to suppress unwanted resonant modes while maintaining good transparency to visible light. The structure consists of graphene sheet on quartz substrate attached to the shielding enclosure made from indium tin oxide. We experimentally demonstrate that the proposed approach can lead to good absorption of microwave waves at a wide frequency range from 5 to 12 GHz and high attenuation of cavity modes up to 20–30 dB. Its effectiveness of EMI shielding averaged 20 dB is proven to be comparable with conventional metallic enclosures. *Published by AIP Publishing.* [<http://dx.doi.org/10.1063/1.4962474>]

Electromagnetic Interference (EMI) to communication systems is problematic with ever-increasing operating frequencies and higher degrees of integration of electronic devices.<sup>1</sup> One of the essential countermeasures is the use of electromagnetic shielding. Efforts have been made over the past two decades to find effective shielding materials such as metals, metallic mesh,<sup>2</sup> doped carbon nanotubes,<sup>3</sup> composite carbon nanotube flexible films,<sup>4</sup> and conducting polymers.<sup>5</sup> By using sol–gel process, inherently conducting polymer based transparent composites have also received superior attention due to their high conductivity and permittivity values.<sup>6,7</sup> However, inherent cavity resonant modes often lead to significant degradation of shielding effectiveness (SE),<sup>8</sup> responsible for unwanted electromagnetic coupling among different electronic components inside the enclosure.<sup>9</sup> With the tendency that an ever-increasing number of electronic components and sub-systems are to be integrated into a limited space, such unwanted coupling of electromagnetic waves may give rise to system malfunction or even failure. Earlier studies have shown that cavity resonant modes can be damped by coating lossy materials onto inner walls of a shielding enclosure.<sup>10</sup> In addition, conductive dielectrics<sup>11</sup> or dielectrics coated with thin resistive films<sup>12</sup> have been used to attenuate cavity resonances. Magnetic thin film,<sup>1</sup> lid of nails,<sup>13</sup> and electromagnetic band gap structures<sup>14</sup> were also applied in recent years.

With optical transparency of up to 97.3%, monolayer graphene films have been found many applications where high optical transparency is essential.<sup>15</sup> With a sheet resistance of the order of 125  $\Omega$ /sq (Ref. 16) to 6000  $\Omega$ /sq,<sup>17</sup> undoped monolayer graphene is able to absorb microwave energy across a wide band of microwave frequencies.<sup>18–22</sup> Following the same principle, we propose a design based on graphene in order to reduce EMIs for electronic systems within the shielding enclosure.<sup>23</sup>

In this letter, we will demonstrate the effectiveness of EM shielding by applying a CVD graphene based design in comparison with its conventional counterpart presented in Ref. 12, where a metallic enclosure (ME) consisting of polyethylene terephthalate (PET) film covered with aluminum foil is used as a reference. Specifically, a monolayer CVD graphene<sup>24</sup> film on quartz substrate is attached to an enclosure made of indium tin oxide (ITO). Suppression effectiveness of two enclosures is demonstrated and compared by both numerical simulations and measurements. A physical insight of EMI reduction mechanism will be discussed.

Cavity resonance modes of a rectangular metallic enclosure will occur at frequencies, which can be determined by<sup>25</sup>

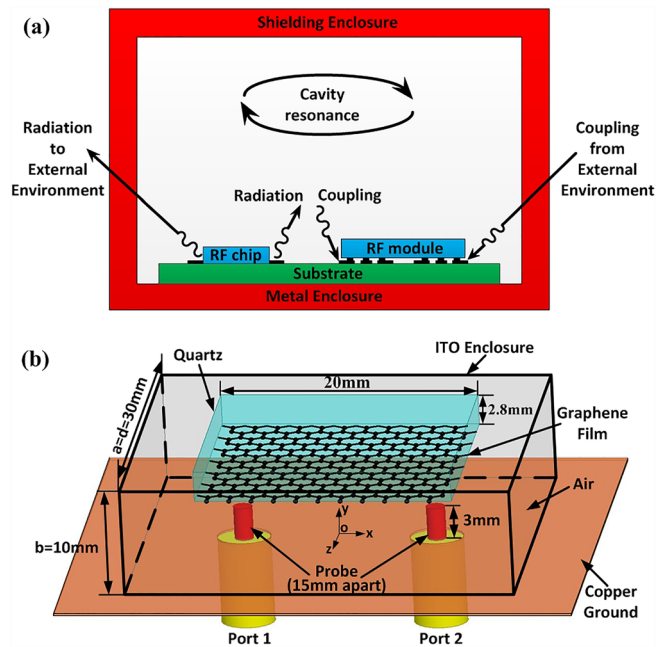


FIG. 1. (a) Various undesired EMI phenomena of packaged microwave module at resonant frequencies. (b) Model of enclosure for simulation and experiment.

<sup>a)</sup>Authors to whom correspondence should be addressed. Electronic addresses: [bwu@mail.xidian.edu.cn](mailto:bwu@mail.xidian.edu.cn) and [y.hao@qmul.ac.uk](mailto:y.hao@qmul.ac.uk)

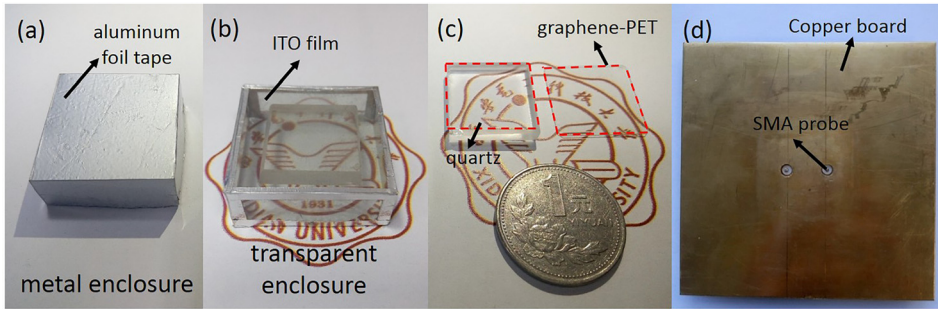


FIG. 2. (a) The rectangular metal enclosure made of aluminum foil tape. (b) The transparent shielding enclosure realized by ITO films. (c) Quartz and CVD graphene (coated on PET) used in the experiment. (d) Schematic of two SMA connectors on a copper board.

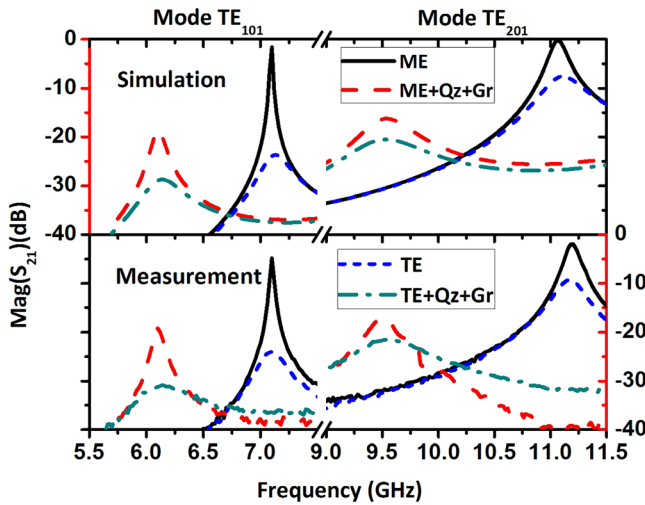


FIG. 3. Simulated and measured transmission coefficients of the metallic enclosure (ME) and ITO transparent enclosure (TE). The status of the two enclosures after graphene (Gr) film and quartz (Qz) imbedded is illustrated.

$$f_{mnl} = \frac{c}{2\pi\sqrt{\mu_r\epsilon_r}} \sqrt{\left(\frac{m\pi}{a}\right)^2 + \left(\frac{n\pi}{b}\right)^2 + \left(\frac{l\pi}{d}\right)^2}, \quad (1)$$

where  $c$  is the speed of light,  $a$ ,  $b$ , and  $d$  are the dimensions of the rectangular cavity,  $m$ ,  $n$ ,  $l$  refer to the number of variations in the standing wave pattern in the  $x$ ,  $y$ ,  $z$  directions, respectively,  $\epsilon_r$  is the relative dielectric constant, and  $\mu_r$  is the relative permeability.

As is illustrated in Fig. 1(a), cavity resonant modes of the metal shielding enclosure can lead to two adverse problems. First, the mutual coupling among different RF modules increases significantly due to the occurrence of cavity modes; second, the SE of the metal enclosure will be reduced, as a result of its strong coupling with EMI.<sup>8</sup>

To solve these two problems simultaneously, cavity resonant modes of shielding enclosure must be damped. What is more, to maintain good optical transparency of the enclosure, materials such as graphene and ITO can be used, as depicted in Fig. 1(b). ITO film with a sheet conductivity of

0.11 S/sq (sheet resistance of 9  $\Omega$ /sq) presented in the proposed design will reflect the EMI<sup>26</sup> from external environment and increase the SE. However, highly reflective cavities made of ITO or other conductive materials often excite unwanted cavity resonant modes in certain frequencies. We anticipate that by utilizing electromagnetic absorbing properties of graphene, a hybrid structure consisting of ITO and graphene can be designed and unwanted electromagnetic resonances can be suppressed. In fact, once the graphene film is attached at the bottom of quartz, surface currents are induced at the graphene layer, this current will be absorbed because of the lossy property of graphene, and this can be used to explain the decrease of resonant intensity.

Experimental apparatus is shown in Fig. 2, a rectangular metallic enclosure made of aluminum foils coated with PET films (Fig. 2(a)) is used as a reference design. Fig. 2(b) presents the proposed shielding enclosure, where an ITO film with a sheet resistance of 9  $\Omega$ /sq is used to form the cavity, while aluminum foil tapes are only used at the joints to ensure good contacts. These two enclosures have the same dimensions as those described in the simulation model shown in Fig. 1(b). Graphene on quartz substrates is attached to the inner walls of the enclosure as shown in Fig. 2(b). Dimensions of the quartz and graphene-PET are 20 mm  $\times$  20 mm  $\times$  2.8 mm and 20 mm  $\times$  20 mm, respectively. In Fig. 2(d), a pair of 3 mm-long SMA connectors is mounted on a copper sheet of size 100 mm  $\times$  100 mm, for the purpose of exciting and measuring resonant cavity modes.

The monolayer graphene film was fabricated by the CVD method before being transferred onto the PET substrates. The sheet resistance of monolayer graphene was measured around 500  $\Omega$ /sq. Resistance discontinuities may occur on the surface of monolayer graphene due to the existence of double layer graphene, wrinkles, and occasional rears. Since the wavelength of the frequencies we studied is much greater than the size of discontinuities point, it has almost no influence on the measured result. And by controlling transfer conditions and post-processing method, scientists can make different graphene samples with diverse sheet resistance.<sup>27–30</sup>

TABLE I. Comparison of measured transmission peaks at resonance.

Mode	Without graphene film		With graphene film	
	Metal enclosure	ITO enclosure	Metal enclosure	ITO enclosure
TE <sub>101</sub>	−4.84 dB at 7.10 GHz	−24.01 dB at 7.10 GHz	−19.15 dB at 6.10 GHz	−30.85 dB at 6.14 GHz
TE <sub>201</sub>	−1.89 dB at 11.20 GHz	−9.24 dB at 11.18 GHz	−16.77 dB at 9.50 GHz	−21.44 dB at 9.54 GHz

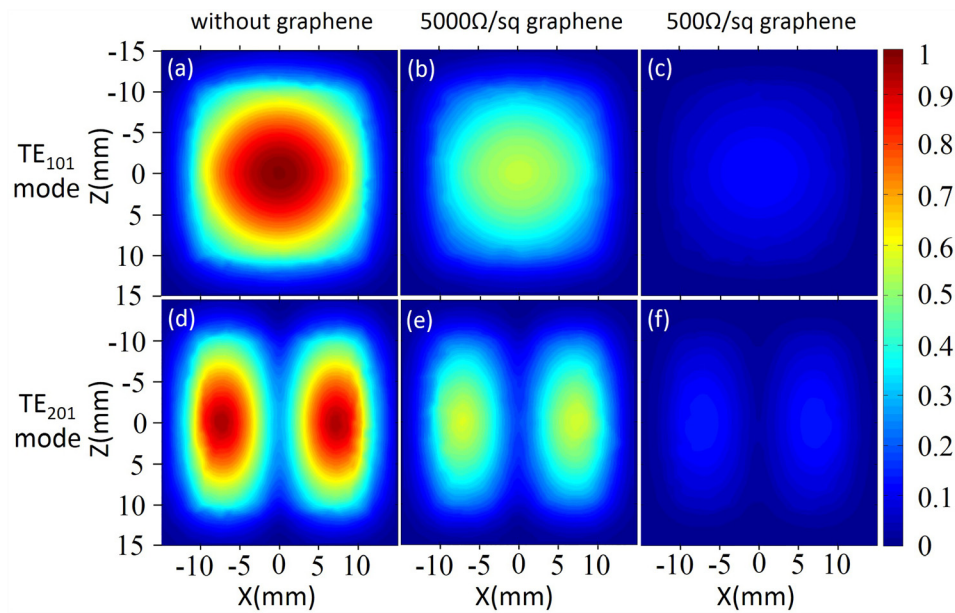


FIG. 4. Contrast contour plot of normalized electric field intensity distribution of ITO enclosure (top view and  $y=6$  mm).  $TE_{101}$  mode ((a)–(c)) and  $TE_{201}$  mode ((d)–(f)) are normalized to 3000 V/m and 6000 V/m, respectively.

Transmission coefficients ( $S_{21}$ ) of both conventional metallic and optically transparent enclosures (TEs) are presented in Fig. 3, showing both simulated and measured results. It is evident that the metal shielding enclosure has two resonant modes ( $TE_{101}$  and  $TE_{201}$ ) at 5.5 GHz and 11.5 GHz, and transmission of both resonant modes is normalized to 0 dB. For the CVD graphene based shielding enclosure, both  $TE_{101}$  and  $TE_{201}$  modes are suppressed by almost 17 dB.

The proposed shielding enclosure in Fig. 2(b) has two major advantages over its metallic counterpart. First, it can be used in electronic systems, where the optical transparency is a required feature. Second, electromagnetic wave absorption from the graphene (with a sheet resistance of  $500 \Omega/\text{sq}$ ) is significant as illustrated in Table I. With the use of graphene, the transmission peak of  $TE_{101}$  mode is decreased by about 15 dB for the metal enclosure and 10 dB more for the ITO enclosure, while for the  $TE_{201}$  mode, the transmission peak is reduced by around 15 dB for the metallic enclosure and 5 dB more for the ITO enclosure. The experiment was carried out by the use of Agilent N9918A vector network analyzer, while simulation results performed using the Ansoft HFSS EM software are in good agreement with measured data.

A closer investigation of electric field distributions within both shielding enclosures reveals that cavity resonant modes can be further suppressed by lowering the sheet resistance of graphene. Fig. 4 shows the contour plot of electric field intensity of the ITO enclosure. Figs. 4(a) and 4(d) show the electric field distributions of the ITO enclosure without graphene on quartz substrates. A graphene film with different sheet resistances has severe effects on the field strength of resonant modes. Figs. 4(b) and 4(e) show that  $TE_{101}$  and  $TE_{201}$  modes of the ITO enclosure will be suppressed with a graphene film of sheet resistance of  $5000 \Omega/\text{sq}$ . They will be further reduced when a sheet resistance of  $500 \Omega/\text{sq}$  is applied as described in Figs. 4(c) and 4(f).

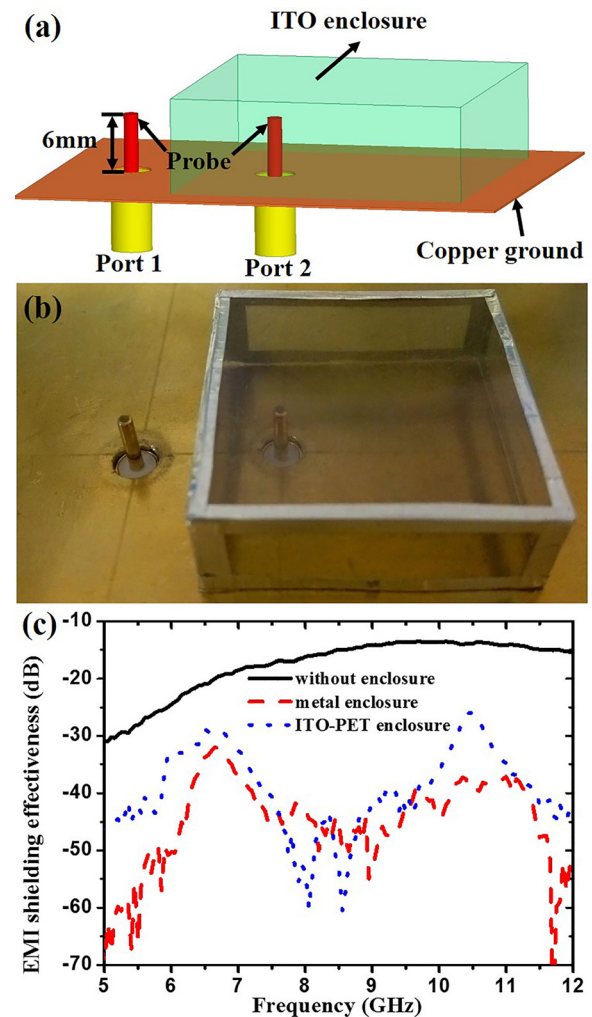


FIG. 5. (a) Schematic of the experimental setup for EMI shielding effectiveness measurement. (b) Physical map of the model shown in (a). (c) Plot of EMI shielding effectiveness for metal enclosure and ITO enclosure, the results without enclosure are displayed for comparison.

It is worth noting that the suppression effectiveness of fundamental mode  $TE_{101}$  is greater than that of  $TE_{201}$ . This can be related to the thickness of graphene/quartz substrate used in the design.

Since the shielding property of the proposed enclosure is determined by ITO film, we measured the SE of the empty enclosure made by ITO film in this section. The ability of EMI shielding can be verified in the experimental setup shown in Figs. 5(a) and 5(b). In this case, the SE is measured by using Agilent N9918A vector network analyzer and the results are shown in Fig. 5(c). It can be noted that the strongest mutual coupling appears around 10 GHz. The conventional metallic enclosure can achieve a good suppression of around 10 dB–40 dB. Performance of the optically transparent enclosure is slightly inferior to that of the metal enclosure, due to its limited conductivity of the ITO film.

In conclusion, we designed an optically transparent shielding enclosure by integrating ITO with graphene/quartz substrates, which effectively suppress cavity resonant modes. The proposed shielding enclosure exhibits good performance from both simulated and measured results. EMI shielding effectiveness of the proposed optically transparent enclosure has been fully demonstrated. This method can be utilized in packaging millimeter-wave integrated hybrid circuits (MICs), monolithic microwave integrated circuits (MMICs), microelectromechanical systems (MEMSs),<sup>31</sup> and other potential applications.

This work was supported by the National Natural Science Foundation of China (Grant No. 61271017), the Natural Science Basic Research Plan in Shaanxi Province of China (Grant No. 2013JZ019), the Fundamental Research Funds for the Central Universities, and the National Key Laboratory Foundation. Some parts of this work were performed at Queen Mary University of London during the visit of BW under the sponsorship of China Scholarship Council (CSC).

<sup>1</sup>J. Sohn, S. H. Han, M. Yamaguchi, and S. H. Lim, *J. Appl. Phys.* **100**, 124510 (2006).

<sup>2</sup>Z. G. Lu, H. Y. Wang, J. B. Tan, and S. Lin, *Appl. Phys. Lett.* **105**, 241904 (2014).

<sup>3</sup>Z. Wang, G. D. Wei, and G. L. Zhao, *Appl. Phys. Lett.* **103**, 183109 (2013).

- <sup>4</sup>Z. P. Wu, D. M. Cheng, W. J. Ma, J. W. Hu, Y. H. Yin, Y. Y. Hu, Y. S. Li, J. G. Yang, and Q. F. Xu, *AIP Adv.* **5**, 067130 (2015).
- <sup>5</sup>R. Kumaran, M. Alagar, S. Dinesh Kumar, V. Subramanian, and K. Dinakaran, *Appl. Phys. Lett.* **107**, 113107 (2015).
- <sup>6</sup>P. Saini, *Fundamentals of Conjugated Polymer Blends, Copolymers and Composites: Synthesis, Properties, and Applications* (John Wiley & Sons, New York, 2015), p. 451.
- <sup>7</sup>R. Kumaran, S. Dinesh Kumar, N. Balasubramanian, M. Alagar, V. Subramanian, and K. Dinakaran, *J. Phys. Chem. C* **120**, 13771 (2016).
- <sup>8</sup>C. Q. Jiao and H. Z. Zhu, *Chin. Phys. B* **22**, 084101 (2013).
- <sup>9</sup>M. J. Chabalko and A. P. Sample, *Appl. Phys. Lett.* **105**, 243902 (2014).
- <sup>10</sup>B. R. Hallford and C. E. Bach, U.S. patent 3,638,148 (1972).
- <sup>11</sup>T. Yamane, A. Nishikata, and Y. Shimizu, *IEEE Trans. Electromagn. Compat.* **42**, 441 (2000).
- <sup>12</sup>D. F. Williams, *IEEE Trans. Microwave Theory Tech.* **37**, 253 (1989).
- <sup>13</sup>A. A. Brazalez, A. U. Zaman, and P. S. Kildal, *IEEE Trans. Compon., Packag., Manuf. Technol.* **2**, 1075 (2012).
- <sup>14</sup>G. Chen and K. L. Melde, *IEEE Trans. Adv. Packag.* **29**, 21 (2006).
- <sup>15</sup>R. R. Nair, P. Blake, A. N. Grigorenko, K. S. Novoselov, T. J. Booth, T. Stauber, N. M. R. Peres, and A. K. Geim, *Science* **320**, 1308 (2008).
- <sup>16</sup>P. Blake, P. D. Brimicombe, R. R. Nair, T. J. Booth, D. Jiang, F. Schedin, L. A. Ponomarenko, S. V. Morozov, H. F. Gleeson, E. W. Hill, A. K. Geim, and K. S. Novoselov, *Nano Lett.* **8**, 1704 (2008).
- <sup>17</sup>S. Bae, H. Kim, Y. Lee, X. Xu, J. S. Park, Y. Zheng, J. Balakrishnan, T. Lei, H. R. Kim, Y. Song, Y. J. Kim, K. S. Kim, B. Özyilmaz, J. H. Ahn, B. H. Hong, and S. Iijima, *Nat. Nanotechnol.* **5**, 574 (2010).
- <sup>18</sup>B. Wu, H. M. Tuncer, M. Naeem, B. Yang, M. T. Cole, W. I. Milne, and Y. Hao, *Sci. Rep.* **4**, 4130 (2014).
- <sup>19</sup>J. Min Woo, M.-S. Kim, H. W. Kim, and J.-H. Jang, *Appl. Phys. Lett.* **104**, 081106 (2014).
- <sup>20</sup>B. Vasić and R. Gajić, *Appl. Phys. Lett.* **103**, 261111 (2013).
- <sup>21</sup>C. Wang, X. J. Han, P. Xu, X. L. Zhang, Y. C. Du, S. R. Hu, J. Y. Wang, and X. H. Wang, *Appl. Phys. Lett.* **98**, 072906 (2011).
- <sup>22</sup>J. P. Wang, Y. Sun, W. Chen, T. Wang, R. X. Xu, and J. Wang, *J. Appl. Phys.* **117**, 154903 (2015).
- <sup>23</sup>B. Wu and Y. Hao, in International Conference on NEMO, Pavia, Italy, 2014.
- <sup>24</sup>Q. Yu, J. Lian, S. Siriponglert, H. Li, Y. P. Chen, and S. S. Pei, *Appl. Phys. Lett.* **93**, 113103 (2008).
- <sup>25</sup>D. Pozar, *Microwave Engineering*, 3rd ed. (Addison-Wesley, Massachusetts, 2005), p. 291.
- <sup>26</sup>R. Gordon, *MRS Bull.* **25**, 52 (2000).
- <sup>27</sup>O. Shaforost, K. Wang, S. Goniszewski, M. Adabi, Z. Guo, S. Hanham, J. Gallop, L. Hao, and N. Klein, *J. Appl. Phys.* **117**, 024501 (2015).
- <sup>28</sup>J. A. Robinson, M. LaBella, M. Zhu, M. Hollander, R. Kasarda, Z. Hughes, K. Trumbull, R. Cavalero, and D. Snyder, *Appl. Phys. Lett.* **98**, 053103 (2011).
- <sup>29</sup>W. Li, Y. R. Liang, D. M. Yu, L. M. Peng, K. P. Pernstich, T. Shen, A. R. Hight Walker, G. G. Cheng, C. A. Hacker, C. A. Richter, Q. L. Li, D. J. Gundlach, and X. L. Liang, *Appl. Phys. Lett.* **102**, 183110 (2013).
- <sup>30</sup>S. Gómez-Díaz, J. Perruisseau-Carrier, P. Sharma, and A. Ionescu, *J. Appl. Phys.* **111**, 114908 (2012).
- <sup>31</sup>A. U. Zaman, M. Alexanderson, T. Vukusic, and P.-S. Kildal, *IEEE Trans. Compon., Packag., Manuf. Technol.* **4**, 16 (2014).